Chemical Geology 493 (2018) 544–552

Contents lists available at ScienceDirect

Chemical Geology

journal homepage: www.elsevier.com/locate/chemgeo

High-precision zirconium stable isotope measurements of geological reference materials as measured by double-spike MC-ICPMS

Edward C. Inglis[a,*], John B. Creech[a], Zhengbin Deng[a], Frédéric Moynier[a,b]

[a] Institut de Physique du Globe de Paris, Sorbonne Paris Cité, Université Paris Diderot, CNRS, 1 rue Jussieu, 75238 Paris cedex 05, France
[b] Institut Universitaire de France, Paris, France

ARTICLE INFO

Editor: K. Mezger

Keywords:
Zirconium
Non-traditional stable isotope
MC-ICPMS
Double-spike
Differentiation
Reference materials

ABSTRACT

Zirconium plays a major role in geochemistry as it is the major cation of zircons - the oldest preserved minerals on Earth. While Zr isotopic anomalies in meteorites have been widely studied, mass dependant Zr stable isotope fractionation during geological processing has been untouched. Here, we report Zr stable isotopic data for terrestrial igneous rocks and present a novel method for the determination of Zr stable isotope ratios within natural geological materials using ion exchange, double-spike, multiple-collector inductively coupled mass spectrometry (MC-ICPMS). Zirconium is isolated from the rock matrix via a chromatographic separation protocol using a first pass column with AG1-X8 anion exchange resin, and a second pass column containing Eichrom® DGA resin. A ^{91}Zr–^{96}Zr double-spike was created from enriched single ^{91}Zr and ^{96}Zr isotope spikes. Samples were combined with the Zr double-spike at a 43:57 spike:sample [Zr] ratio, prior to dissolution and column chemistry. After column chemistry the purified sample solutions were analysed on a Thermo Scientific Neptune Plus MC-ICPMS and the data was reduced using *IsoSpike*, with the final Zr isotope data being reported as the per mil deviation of the ^{94}Zr/^{90}Zr from the IPGP-Zr standard ($\delta^{94/90}Zr_{IPGP\text{-}Zr}$). The $\delta^{94/90}Zr_{IPGP\text{-}Zr}$ of six igneous standard reference materials: two basalts (BHVO-2 and JB-2), one andesite (AGV-2), two granites (GA and GS-N) and a serpentinite (UB-N) as well as one individual zircon grain (Plešovice zircon), are presented using this method. Sample measurements are presented with an analytical uncertainty of ± ~0.05‰ (2*sd*) for $\delta^{94/90}Zr_{IPGP\text{-}Zr}$ and these rocks exhibit isotopic variations of ~0.15‰ for $\delta^{94/90}Zr_{IPGP\text{-}Zr}$. These results demonstrate that natural variations of Zr isotopes occur within terrestrial igneous rocks, and are resolvable with this method. Finally the variation of $\delta^{94/90}Zr_{IPGP\text{-}Zr}$ values observed within the magmatic rock reference materials is correlated ($R^2 = 0.78$; $n = 5$) with SiO_2, suggesting that Zr isotopes could serve as a sensitive tracer of magmatic processes.

1. Introduction

The age of plasma-source multiple collection mass spectrometry has seen a relative boom in the number of different stable isotope systems that have been developed and applied to solve various geo- and cosmochemical problems over the last two decades (see review by Teng et al., 2017). While relatively mature stable isotope systems continue to provide powerful constraints on various natural processes, the development and subsequent application of new systems is needed in order to constrain different earth and planetary processes.

High-field strength elements (HFSEs) have been extensively studied within the field of high-temperature geochemistry. These elements are classified on the basis of exhibiting a small ionic radii (*Z*) relative to a high cationic charge (*r*), and although all elements displaying a $Z/r > 2$ are considered high-field strength (Rollinson, 1993), this classification has traditionally been applied to Hf, Zr, Ti, Nb and Ta within a geological context (Salters, 1998). Owing to their high *Z/r* ratio, the HFSEs are not readily incorporated in the crystal lattice of most mantle minerals, and, as such, behave as incompatible elements during mantle melting events (e.g. Salters and Shimizu, 1988). Furthermore, they are generally considered poorly mobile in low pressure aqueous fluids and, as such, are comparatively resistant to late metamorphic and alteration effects (Winchester and Floyd, 1977). Consequently the HFSEs serve as good tools to trace historic mantle depletion events and the petrogenesis of igneous rocks (e.g. Kelemen, 1990; Woodhead et al., 1993; Niu, 1997, 2004; van Westrenen et al., 2001; Weyer et al., 2003).

Despite their unique geochemical behaviour, the HFSEs have received relatively little attention in terms of stable isotope geochemistry. Only Ti has been extensively investigated for mass-dependant stable

* Corresponding author.
E-mail address: inglis@ipgp.fr (E.C. Inglis).

https://doi.org/10.1016/j.chemgeo.2018.07.007
Received 26 March 2018; Received in revised form 4 July 2018; Accepted 8 July 2018
Available online 18 July 2018

isotope variations in nature (e.g. Millet et al., 2016). Zirconium is a key member of the HFSE group and occurs as a transition metal, d-block element within the periodic table. It behaves as a refractory incompatible element during partial melting of Earth's mantle, and is consequently enriched in the crust ($> 100\,\mu g\,g^{-1}$; Ronov and Yaroshevsky, 1969) relative to bulk silicate earth ($\sim 10\,\mu g\,g^{-1}$; McDonough and Sun, 1995). Zirconium has five stable isotopes: ^{90}Zr (51.45%); ^{91}Zr (11.22%); ^{92}Zr (17.15%); ^{94}Zr (17.38%); ^{96}Zr (2.80%), thus making it an interesting target for examining mass-dependent stable isotope variations within geological processes. Additionally, as Zr has more than four stable isotopes, it is a suitable candidate for the application of the double spike technique to discriminate for processing or analytically induced mass bias effects. Zirconium isotopes have been studied before but largely from a mass independent perspective (e.g. Schönbächler et al., 2004; Iizuka et al., 2016), although Akram & Schönbächler (2016) did examine a selection of synthetic standards and geo-reference materials and documented a range of mass dependent isotopic variations.

Recently, non-traditional stable isotopes have served as a powerful tool to study igneous differentiation and the temporal and spatial evolution of Earth's mantle (e.g. Dauphas et al., 2009; Chen et al., 2013; Millet et al., 2016; Greber et al., 2017a, 2017b). Because Zr is among one of the most refractory trace elements found on Earth it is comparatively resistant to evaporation and condensation, metamorphism and late alteration, thus making it relatively easy to understand primary igneous processes. Furthermore, seeing as the highly refractory mineral zircon represent a major host of Zr, it is possible that Zr isotopes could serve as a powerful tracer for understanding the evolution of source and growth of continental crust through time, without suffering from the effects of metamorphism and alteration that other stable isotope systems are susceptible to.

Here we present data for one zircon mineral separate reference material and six terrestrial silicate rocks and explore the utility of Zr isotopes as tracers of igneous processes on Earth. A new analytical method for the determination of high precision ($< \pm 0.05$‰, 2*sd*) Zr isotope ratios within terrestrial silicate rock and mineral separate samples is also presented in detail.

2. Double-spike preparation and calibration

The double-spike technique is a well-established method for the determination of high-precision isotope ratios in various earth and planetary materials. The advantages of the double-spike technique have been known since early measurements of radiogenic isotope ratios by thermal ionization instruments (TIMS; Compston and Oversby, 1969; Gale, 1970; Dodson, 1970; Russell, 1971; Cumming, 1973). More recently, the application of the double-spike technique has been extended to generate high-precision ratios of non-traditional stable isotope systems by multiple-collector inductively couple plasma mass spectrometers (MC-ICPMS; e.g., Siebert et al., 2001, 2006; Gopalan et al., 2006; Weyer et al., 2008; Schoenberg et al., 2008; Mead and Johnson, 2010; Arnold et al., 2010; Bonnand et al., 2011; Xue et al., 2012; Millet et al., 2012; Millet and Dauphas, 2014; Gall et al., 2012; Creech et al., 2013, 2017; Pogge von Strandmann et al., 2014; Hopp et al., 2016; Nanne et al., 2017; McCoy-West et al., 2017; Deng et al., 2018). The double-spike approach is recognised as the only means to correct mass discrimination effects that can be encountered during sample dissolution, ion exchange chromatography and/or mass spectrometry.

The design of the double-spike used in this study was determined based on minimum theoretical errors calculated using the double-spike toolbox of Rudge et al. (2009). As such, a ^{91}Zr–^{96}Zr double-spike was prepared and ^{90}Zr–^{91}Zr–^{94}Zr–^{96}Zr were used in the double-spike inversion, as this combination is predicted to have the minimum theoretical error on double-spike corrected ratios (ca. 18 ppm/amu; Rudge et al., 2009), and to be accurate over a broad range of sample–spike mixing proportions. Two single isotope Zr spikes, ^{91}Zr and ^{96}Zr, were obtained from Isoflex (www.isoflex.com). The procedures used for the dissolution and calibration of the isotopic compositions of the single spikes and for the preparation and calibration of the isotopic composition of the double-spike are presented below.

3. Materials and methods

3.1. Reagents, standards and reference materials

All laboratory work was carried out within class 100 laminar flow workstations as part of the clean geochemistry facility at the Institute de Physique du Globe de Paris (IPGP). Concentrated reagents (HCl, HNO_3, HF) were purchased from BASF France as Selectipur® grade, and were further purified by sub-boiling distillation using Savillex™ Teflon stills. All further dilutions of reagents were performed using 18.2 MΩ cm ultra-pure H_2O from a Merk™ Millipore Milli-Q® (MQ) purification system.

As no Zr isotope reference material is presently available, the Zr isotope standard used for mass spectrometry was produced from a PlasmaCal™ 1000 $\mu g\,mL^{-1}$ ICP standard (Lot: 5131203028, 2015). This solution is hereafter referred to as IPGP-Zr, and is available for distribution to other laboratories on request by contacting the corresponding author.

Six different whole rock reference materials with Zr concentrations ranging between 4 and 235 $\mu g\,g^{-1}$, were selected for characterisation of the range of Zr isotope variation within terrestrial igneous rocks. These comprised: two basalts (JB-2; Geological Survey of Japan [GSJ], BHVO-2; United States Geological Survey [USGS]); two granites (GA and GS-N; Service d'Analyse des Roches et des Minéraux [SARM]); one andesite (AGV-2; USGS), and; one serpentinised peridotite (UB-N; SARM). In addition we also obtained several grains of Plešovice zircon (Sláma et al., 2008), which represents a 337.13 ± 0.37 Ma zircon grain found within a potassic granulite from the Bohemian Massif (Czech Republic).

3.2. Sample dissolution

Because much of the Zr within igneous rocks is likely to be hosted within refractory zircon grains, it was decided that comparison between different dissolution methods would be required. For this two dissolution methods were selected:

1) *Teflon bombs* – This method involves the digestion of between 20 and 100 mg of rock powder by the addition of 2 mL concentrated HF (29 M) and 2 mL HNO_3 (16 M) acids at a 1:2 ratio within Savillex® standard square bodied PFA Teflon vials (herein referred to as Teflon bombs). Teflon vials are sealed using a wrench top closure and Ultem® socket cap in order to prevent breach of the seal when the vial is heated to high temperatures. The sealed vials are placed within a high wall Teflon coated hotplate and heated to 165 °C for 5 days.
2) *Parr bombs* – This method follows a well-established protocol (e.g. Navarro et al., 2008). Sample digestion by this method sees the sample material placed within a PTFE vial in combination with 2 mL concentrated HF (29 M) and 2 mL HNO_3 (16 M) acids at a 1:2 ratio. These PTFE vials are then placed within a spring loaded screw-top steel vessel. The combined assembly is then heated in an oven at 150 °C for 5 days.

To examine the effectiveness of each method for Zr isotopes, we tested dissolutions of whole rock powder (GA) and individual Plešovice zircon grains. Approximately 50 mg of GA sample powder was weighed directly into the digestion vessels and was double-spiked at the correct proportion. For the Plešovice zircon, two individual grains were selected, weighed and added (uncrushed) to separate digestion vessels. Because of the high total Zr concentration of these samples, an unrealistically large volume of Zr double-spike would be required in order

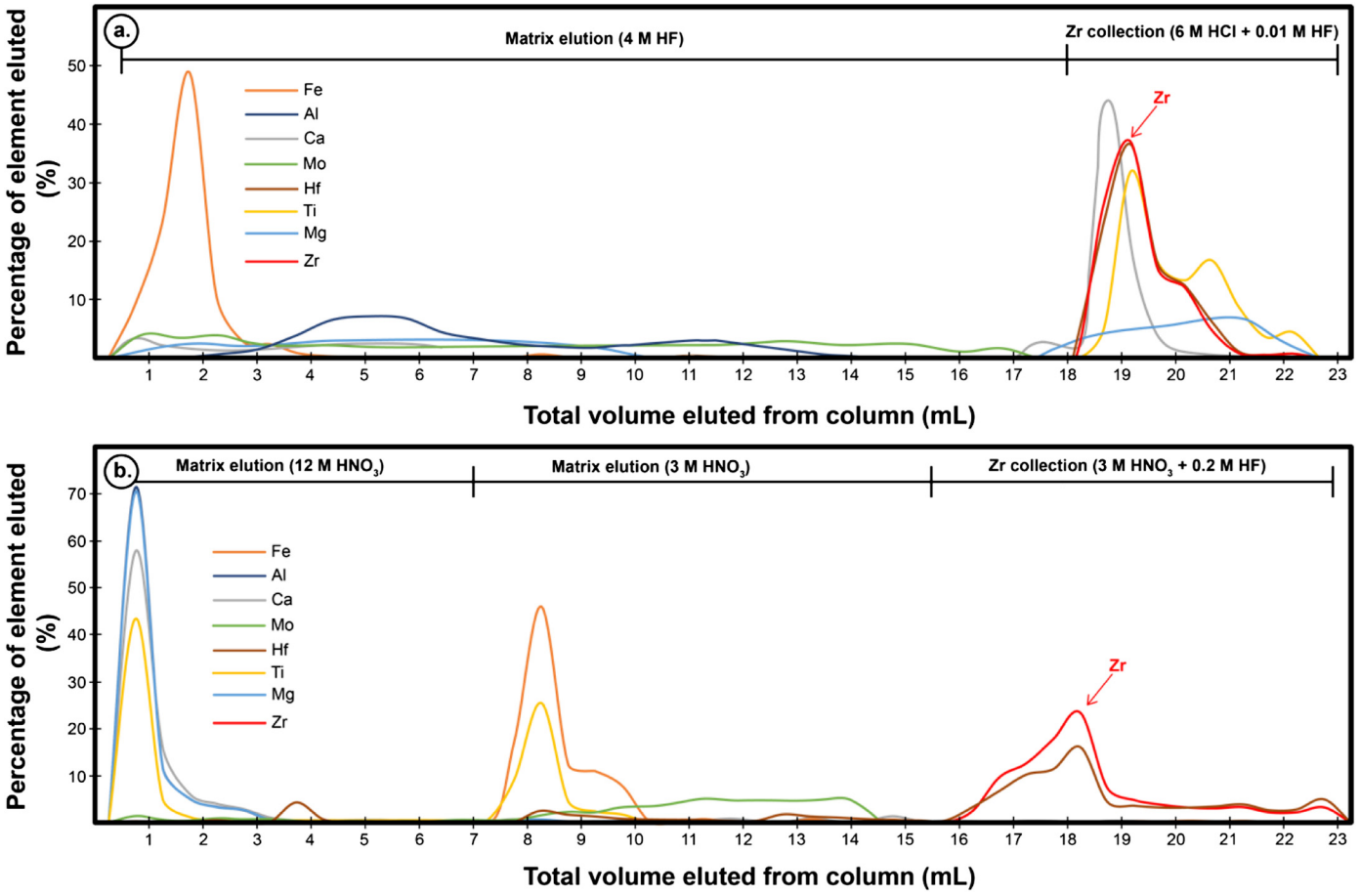

Fig. 1. Representative elution profiles for the ion exchange protocol used here to isolate Zr from matrix elements. The elution profiles here are for BHVO-2. The top panel (a.) shows the elution profile for BHVO-2 on the first stage AG1-X8 column. The bottom panel (b.) shows the elution profile for BHVO-2 on the second stage DGA column.

to spike these samples at the right proportion. As such, the Plešovice zircons were left unspiked until after dissolution and dilution, prior to mass spectrometry as these samples did not require Zr separation by column chemistry.

3.3. Ion exchange chromatography

In order to isolate Zr from the sample matrix a new ion exchange protocol has been developed. This method utilises a two-step procedure on separate AG1-X8 and DGA columns. The elution profiles for both of these columns are shown in Fig. 1. The combined Zr yield for this chemistry procedure is ~70% for BHVO2.

3.3.1. First stage AG 1-X8 column

This first step column is designed to provide sufficient isolation of Zr from the major elements within the sample matrix (Fe, Al, Ca, Mg, Cr) as well as Mo, the latter of which has direct isobaric interferences on ^{92}Zr, ^{94}Zr and ^{96}Zr from ^{92}Mo, ^{94}Mo and ^{96}Mo. The first ion exchange column follows that of Schönbächler et al. (2004) with some modification as described below.

The first stage column is performed by using a Poly-Prep® column obtained from Bio-Rad (USA). This column has a conical resin bed of 4 × 0.8 cm, capable of holding up to 2 mL of resin, and a large associated reservoir. The resin used for this step was the anionic chloride form Bio-Rad AG 1-X8 (200–400 mesh size). The full procedural steps for this part of the chemistry are given in Table 1a.

Prior to loading on the column, samples were dried down from the initial HF-HNO_3 step used for sample decomposition. Because the use of HF is well known to promote the formation of poorly soluble fluoride complexes, which readily sequester HFSEs (e.g. Kleinhanns et al., 2002), it was vital that all of these were brought fully into solution. This was achieved by refluxing samples in 2 mL of 6 M HCl at 165 °C in Teflon bombs for 48 h, evaporating to dryness and further refluxing in 16 M HNO_3 at 165 °C for 48 h. After these reflux steps all sample solutions were completely clear and it was deemed that all fluoride complexes had been brought fully solution. These solutions were evaporated to dryness and brought back into solution in 2 mL of 4 M HF. Because HF is not particularly effective at re-dissolving silicate sample residues it was necessary to do this in two stages. First 1 mL of HF was added to the sample residue, which was in turn heated to 125 °C for 3 h before being placed in an ultrasonic bath for 1 h, this solution was then centrifuged and the supernatant decanted into a clean Teflon beaker. The remaining sample residue was transferred back into the original sample Teflon beaker by the addition of 1 mL of 4 M HF. This was then heated on the hotplate at 125 °C for 3 h and then agitated in the ultrasonic bath for a further hour. This sample solution was centrifuged and the supernatant removed from the small amount of remaining residue. Finally both supernatant cuts were combined ready for loading onto the column. This method of HF solution preparation has been demonstrated to effectively increase the yield of Zr from similar column chemistries (Schönbächler et al., 2004).

The Bio-Rad Poly-Prep columns were loaded with 2 mL of AG1-X8 (200–400 mesh size) which was then pre-cleaned on the column by addition of 6 mL 2 M HNO_3, 6 mL Milli-Q (MQ) H_2O, 6 mL 6 M HCl + 0.01 M HF and 6 mL MQ. The resin was preconditioned with 8 mL of 4 M HF before the 2 mL of sample solution was added. The

Table 1
Column chemistry procedure for Zr separation used in this study. Table 1a. shows the procedure for the first stage column using AG1 X8 resin (200–400 mesh) on a BioRad PolyPrep column. Table 1b. shows the procedure for the second stage column using DGA resin on a BioRad PolyPrep column.

a. First stage column (AG1-X8)

Step	Reagent	Volume (mL)
Resin cleaning	2 M HNO_3	6
	MQ H_2O	6
	6 M HCl + 0.01 M HF	6
Precondition	4 M HF	4
	4 M HF	4
Sample load	4 M HF	2
Matrix elution	4 M HF	4.5
	4 M HF	4.5
	4 M HF	4.5
	4 M HF	4.5
Sample elution	6 M HCl + 0.01 M HF	5

b. Second stage column (DGA)

Step	Reagent	Volume (mL)
Resin cleaning	MQ H_2O	6
	12 M HNO_3	6
	3 M HNO_3 + 0.2 M HF	6
Precondition	12 M HNO_3	2
	12 M HNO_3	2
Sample load	12 M HNO_3	1
Matrix elution	12 M HNO_3	3.5
	12 M HNO_3	3.5
	3 M HNO_3	4
	3 M HNO_3	4
Sample elution	3 M HNO_3 + 0.2 M HF	3.5
	3 M HNO_3 + 0.2 M HF	3.5

matrix was washed from the column by the total addition of 18 mL of 4 M HF. Finally Zr (and other HFSEs) were eluted from the column in a total of 5 mL of 6 M HCl + 0.01 M HF. This cut was collected into a clean Teflon beaker and evaporated to dryness ready for the second stage column chemistry. After chemistry, the resin was cleaned using the same procedure described before. A typical elution profile for this column chemistry is shown in Fig. 1a.

3.3.2. Second stage DGA column

The second stage chemistry is specifically designed to further purify the Zr fraction, particularly from Ti, which is eluted alongside Zr during the first stage column. This chromatographic separation is performed on a Bio-Rad Poly-Prep column using Eichrom N,N,N′,N′-tetra-n-octyl-diglycolamide (DGA) 50–100 μm particle size resin. The full procedural steps for this second stage chemistry are summarised in Table 1b.

The dried sample fractions obtained from the first stage chemistry were brought fully into solution in 1 mL of 12 M HNO_3. The Poly-Prep columns were loaded with 2 mL of DGA resin, which was subsequently cleaned on the column with repeated passes of MQ H_2O, 12 M HNO_3 and 3 M HNO_3 + 0.2 M HF. The resin was preconditioned with 4 mL of 12 M HNO3 before loading sample solutions. Two different molarities of HNO_3 were used to wash the remaining matrix from the Zr fractions; firstly 7 mL of 12 M HNO_3 was added followed by 8 mL of 3 M HNO_3. The recovery of Zr into clean Teflon beakers was then achieved by the addition of 7 mL of 3 M HNO_3 + 0.2 M HF. As before the resin was cleaned on the column using the same pre-cleaning steps outlined prior to preconditioning and sample loading. The elution profile for this column chemistry is shown in Fig. 1b.

3.4. Mass spectrometry

All Zr isotope measurements presented were carried out on a Thermo Scientific® Neptune Plus Multiple-Collector Inductively Coupled Plasma Source Mass Spectrometer (MC-ICPMS) at the Institut de Physique du Globe de Paris. The instrument operating conditions are provided in the Supplementary Information Table S1. Sample and standard solutions were prepared at 200 ng mL^{-1} total Zr in 0.5 M HNO_3. All of the bulk rock samples were spiked prior to initial sample digestion, while the Plešovice zircon samples were further diluted and spiked in the correct proportion prior to mass spectrometry.

Samples were introduced to the instrument via an Elemental Scientific Instruments (ESI) PFA-50 (~50 μl min^{-1}) self-aspirating nebuliser and associated sample capillary. This nebuliser was connected to an ESI Apex-IR desolvating sample introduction system, which was in turn coupled directly to the injector interface of the quartz torch assembly. Nickel Jet Sample and H Skimmer interface cones were used and the instrument was run in low mass resolution mode, which gave a mass resolution (mass/Δmass at 95% and 5% of the low mass side leading peak edge) of ~1600. The selected ion beams were collected in the movable faraday detectors mounted in the back end of the instrument. These detectors were all connected to 10^{11} Ω pre-gain amplifiers, which were calibrated at the beginning of each analytical session. All masses of Zr were collected ($^{90}Zr^+$, $^{91}Zr^+$, $^{92}Zr^+$, $^{94}Zr^+$ and $^{96}Zr^+$) alongside $^{88}Sr^+$ and $^{95}Mo^+$ - the latter in order to monitor for interferences of $^{94}Mo^+$ and $^{96}Mo^+$ on $^{94}Zr^+$ and $^{96}Zr^+$ respectively. When parameterised according to the operating conditions given in Supplementary Information Table S1 and optimally tuned for sensitivity this configuration gave a total combined beam intensity for Zr of ~60 V for a 200 ng mL^{-1} total Zr solution.

Each sample measurement consisted of a block of 50 integrations each lasting 4.194 s. Baseline corrections were performed by subtracting on-peak zeros that were measured in clean 0.5 M HNO_3 prior to each sample analysis. Post measurement wash-outs were performed for 10 min in order to return to pre analysis background beam intensities. Each sample was analysed 4 times throughout the session. The IPGP-Zr standard was analysed after every 4 measurements of individual samples. Data was reduced via a series of double-spike inversion calculations using the double-spike data reduction tool *IsoSpike* (Creech and Paul, 2015). All data is reported in delta notation as $\delta^{94/90}Zr_{IPGP\text{-}Zr}$, which represents the deviation of the $^{94}Zr/^{90}Zr$ ratio of a sample relative to the same ratio in the IPGP-Zr standard solution in parts per thousand (‰) (Eq. (1)).

$$\delta^{94/90}Zr_{IPGP-Zr} = \left(\frac{\left(\frac{^{94}Zr}{^{90}Zr}\right)_{sample}}{\left(\frac{^{94}Zr}{^{90}Zr}\right)_{IPGP-Zr}} - 1 \right) \times 1000 \quad (1)$$

3.5. Preparation of the ^{91}Zr–^{96}Zr double-spike

3.5.1. Digestion and calibration of single spikes

Two single isotope Zr spikes, ^{91}Zr and ^{96}Zr, were obtained from Isoflex (www.isoflex.com); the ^{91}Zr spike was provided in a metallic form, while the ^{96}Zr spike was provided as an oxide powder. The spikes were carefully weighed and transferred to PFA Teflon bottles for digestion. To each spike, 10 mL of 6 M HCl + 1 M HF was added, and the bottles were then placed on a hotplate at 120 °C for 24 h, after which the spikes were fully in solution. The spikes were then evaporated to dryness, and re-dissolved in a volume of 0.5 M HNO_3 + 0.01 M HF for an ideal concentration (based on weight) of 1000 μg mL^{-1} for storage. Aliquots of each spike were taken for calibration by MC-ICPMS. Spike compositions were calibrated in two ways: 1) by bracketing with analyses of the IPGP-Zr standard and assuming the natural Zr isotope composition from Berglund and Wieser (2011); and 2) by doping with a small amount of Sr, using an alternate collector configuration permitting collection of ^{87}Sr and ^{88}Sr in the same cycle as all Zr isotopes, and normalising measured ratios such that the $^{87}Sr/^{88}Sr = 11.79714$ based

on the natural abundance ratio from Berglund and Wieser (2011). Optimal isotope dilution mixtures of the Zr standard and each spike were also prepared, and the known quantity of Zr from the standard was used to perform a reverse isotope dilution calculation to accurately determine the concentration of each spike solution.

3.5.2. Mixing and calibration of the ^{91}Zr–^{96}Zr double-spike

Using the calibrated compositions for each single isotope spike, the optimal double-spike mixture composition was calculated using the double-spike toolbox of Rudge et al. (2009). Based on these simulations, the optimal double-spike mixture was determined to be 51.4% ^{91}Zr and 48.6% ^{96}Zr, with an optimal ^{91}Zr–^{96}Zr double-spike to sample ratio of 43:57, and using ^{90}Zr–^{91}Zr–^{94}Zr–^{96}Zr in the double-spike inversion. The double-spike was prepared by mixing the calibrated single-spikes in the given proportions, and diluted in a solution of 0.5 M HNO_3 + 0.01 M HF to have a total Zr concentration of 250 μg mL^{-1}.

The ^{91}Zr–^{96}Zr double-spike was calibrated by making repeated analyses (n = 20) of the double-spike bracketed by analyses of the IPGP-Zr standard. The accuracy of the calibration was tested by analysing a set of double-spike–IPGP-Zr mixtures with proportions of double-spike in the mixture ranging from 0.15–0.80 (equivalent to standard/spike ratio of 5.7–0.3, or 0.35–1.86 times the optimal double-spike fraction). The results of these analyses are shown in Fig. 2. Across the range of mixtures tested those within the range ~0.38–~0.58 double spike to sample yield delta values ($\delta^{94/90}Zr_{IPGP\text{-}Zr}$) within typical uncertainty (i.e., ± 0.04‰; see below) of zero, while samples below and above this range can give values which are offset outside of uncertainty from zero. This is in excellent agreement with the spike:-sample proportion plateau calculated using the double-spike tool box of Rudge et al. (2009).

4. Results and discussion

4.1. Comparison of different sample dissolution techniques

Because a large fraction of the Zr within igneous rocks is likely to be hosted within highly refractory zircon grains it was necessary to examine the effectiveness of different dissolution techniques for Zr isotopes. As described in Section 3.2 multiple dissolutions using either Teflon or Parr bombs have been performed on the GA whole rock

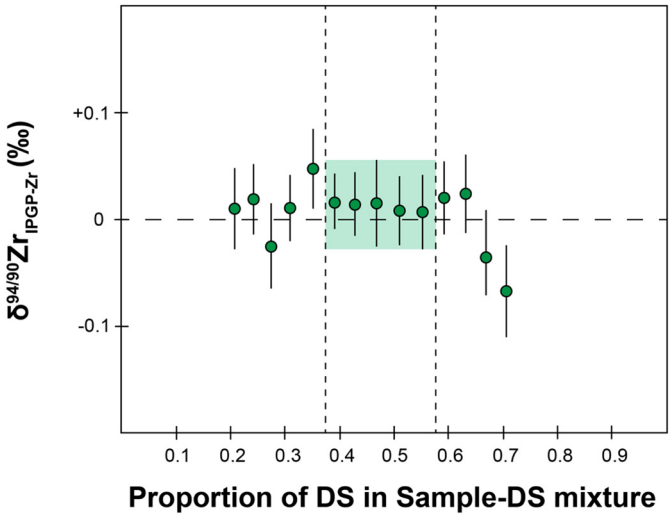

Fig. 2. A plot showing the results of sample-double spike (DS) mixing calibrations. The dashed vertical lines and green box show the range of sample-DS mixtures that are deemed acceptable. All uncertainties on individual data points represent the internal 2× standard error (2se) of one individual measurement. (For interpretation of the references to colour in this figure legend, the reader is referred to the web version of this article.)

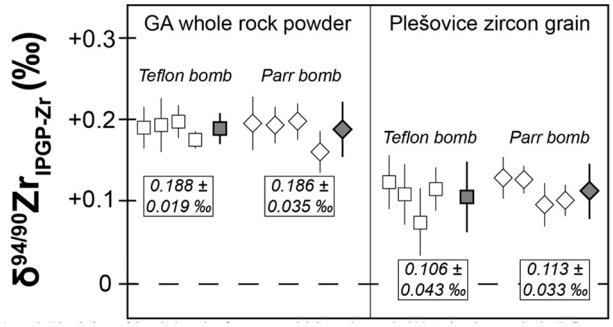

Fig. 3. Dissolutions of the whole rock reference material GA and uncrushed Plešovice zircon grains by Teflon (square symbols) and Parr bomb (diamond symbols). Individual sample measurements are shown as hollow symbols and the associated uncertainties of these points is the internal 2se of each individual measurement. Filled symbols represent the mean of the 4 individual measurements and the uncertainty of these points is the 2sd of the four measurements used to calculate the mean.

powder and on uncrushed grains of the Plešovice zircon.

The $\delta^{94/90}Zr_{IPGP\text{-}Zr}$ values for four individual measurements of the granitic whole rock reference material GA and uncrushed Plešovice zircon grains, which were both digested by Teflon bomb and Parr bomb methods, are reported in Fig. 3. Each sample aliquot was analysed four times throughout the same analytical session. The value discussed in text is the average and two times the standard deviation of these values. The granite GA digested by Teflon bomb yielded an average $\delta^{94/90}Zr_{IPGP\text{-}Zr}$ value of 0.188 ± 0.019‰, while the powder digested using the Parr bomb technique gave an average $\delta^{94/90}Zr_{IPGP\text{-}Zr}$ value of 0.186 ± 0.035‰. For the Plešovice zircon grains the sample digested by Teflon bomb had an average $\delta^{94/90}Zr_{IPGP\text{-}Zr}$ value of 0.106 ± 0.043‰ and the grain dissolved in the Parr bomb had an average $\delta^{94/90}Zr_{IPGP\text{-}Zr}$ value of 0.113 ± 0.033‰.

It is apparent that the dissolution of these samples by Parr and Teflon bombs yield Zr isotopic compositions for both that are unresolvable from one another. This implies that the use of widely available Teflon bombs is a robust and reliable method for sample dissolution for the analysis of Zr stable isotopes.

4.2. Spectral interferences, matrix effects and Zr concentration

Spectral or isobaric mass interferences are a constant source of error encountered for both concentration and isotope ratio data obtained by plasma sourced mass spectrometry (e.g. May and Wiedmeyer, 1998). Such interferences can occur when the nominal mass space of a given analyte isotope is blocked or interfered by monoatomic, polyatomic or doubly charged species of another element or elements. Different solutions to the problem are commonly implemented including the use of variable mass resolution in order to resolve the interference from the analyte (e.g. Weyer and Schwieters, 2003) and front end collision cells to combine the interfering elements with a reaction gas and shift it away for the mass spectrum of interest (e.g. Boulyga and Becker, 2001). Of particular concern is the direct monoatomic interference potential of charged Mo, of which $^{92}Mo^+$ (14.84%), $^{94}Mo^+$ (9.25%) and $^{96}Mo^+$ (16.68%) occupy the same nominal mass space as $^{92}Zr^+$, $^{94}Zr^+$ and $^{96}Zr^+$. Indeed the results of different inter-element doping tests presented in Fig. 4 show that even with the addition of a relatively small amount of Mo (1% Mo of total sample solution) can perturb the $\delta^{94/90}Zr_{IPGP\text{-}Zr}$ values of the standard solution towards erroneously light values. In light of this result, it is of critical importance to ensure that all Zr fractions are virtually free from Mo. The column chemistry procedure described in Section 3.3 and the associated elution profiles (Fig. 1a and b) demonstrate that effective separation of Mo from the Zr sample cut is achieved. In order to ensure that no Mo is present in the sample solutions after column chemistry, during mass spectrometry $^{95}Mo^+$ is

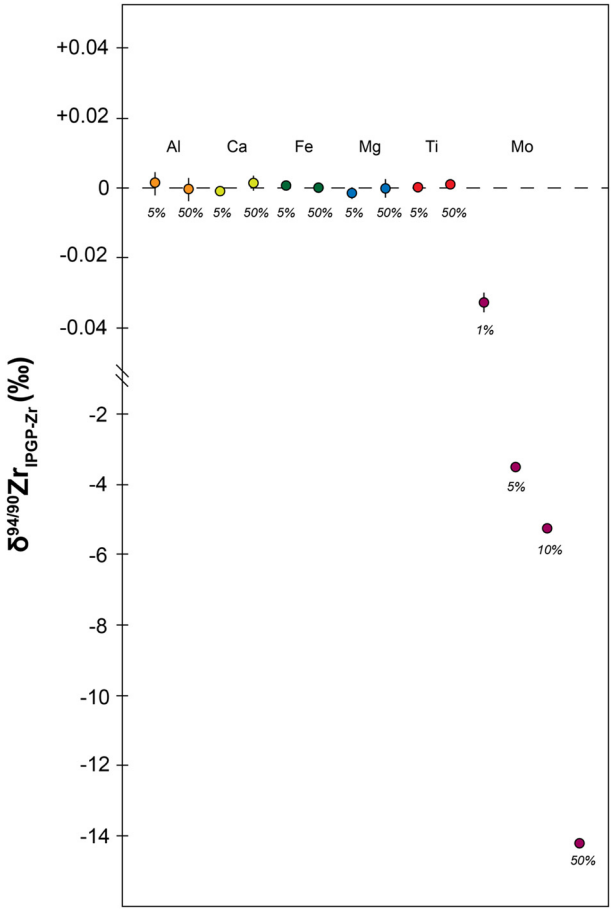

Fig. 4. The effect of inter element doping of the pure IPGP-Zr standard solution. For Al, Ca, Fe, Mg and Ti the two circle symbols represent doping of the given element at 5 and 10% relative to the total [Zr] (i.e [x]:[Zr] of 0.1:1 and 1:1 when x represents the dopant element). For Mo doping is at 1, 5, 10 and 50% increments. The uncertainties on sample symbols are the 2sd of the mean when $n = 3$.

monitored alongside all of the Zr masses. In the case for all samples analysed as part of this study it was found that the sample solutions never contained > 0.01 ng (equivalent to a Mo:Zr ratio of 0.0001:1), which is comparable to the amount of Mo within the pure standard solution analysed alongside the samples. In addition to the potential monoatomic interferences of Mo, the polyatomic $^{50}Ti^{40}Ar^{+}$ species could also interfere on $^{90}Zr^{+}$ (Schönbächler et al., 2004). To test this, pure IPGP-Zr standard solutions were doped with 5% and 50% elemental Ti, the results of which are shown in Fig. 4. Even at a Ti:Zr of 1:1 the $\delta^{94/90}Zr_{IPGP\text{-}Zr}$ value were not biased, suggesting that the presence of the Ti argide is insignificant compared to the contribution from $^{90}Zr^{+}$, and that the Zr separation technique described here effectively isolates Zr from Ti in the sample matrix. Additionally, because ^{96}Zr is used as one of the spike isotopes, it is important to correct for any polyatomic species, such as $^{56}Fe^{40}Ar^{+}$ that may be present in the nominal 96 mass space. The effect of Fe has been examined using the same approach as for Ti. Much like Ti, the results for the standard solution show no apparent deviation from the 0 value even with a Fe:Zr ratio of 1:1, ultimately demonstrating that the Fe argide is insignificant relative to $^{96}Zr^{+}$. The possible interference from ^{40}Ar-^{40}Ar-^{16}O was monitored during the baseline measurements and was found to be subordinate to the noise of the amplifier (signal under 0.4 mV for the 96 mass space) and therefore negligible one compared to the ^{96}Zr signal (> 16 V).

In addition to issues relating to spectral interferences, the problem of matrix effects can strongly bias isotope ratio measurements of samples analysed by plasma source instruments (e.g. Shiel et al., 2009). These effects are relatively poorly understood, but collectively refer to changes in the operating behaviour of the mass spectrometer, such as suppression of ionization efficiency and non-linear shifts in the instrumental mass bias (Rehkämper et al., 2004; Carlson et al., 2001; Galy et al., 2001; Ingle et al., 2003; Chaussidon et al., 2017). To ensure that this method was not susceptible to such matrix effects a series of doping tests were conducted, the results of which are presented in Fig. 4. Varying contributions of between 5% and 10% (up to 50% for Ti) of different matrix elements (i.e., [X]/[Zr], where X represents the dopants Al, Ca, Fe, Mg and Ti and [Zr] is the amount of Zr within the standard solution) produce no resolvable deviation of the $\delta^{94/90}Zr_{IPGP\text{-}Zr}$ values from the idealised absolute zero value (Fig. 4). As such, it is apparent that the effects of different matrix contaminants within the Zr analyte solutions are corrected by the double-spike method.

Alongside examining the role of spectral interferences and matrix effect, a series of tests relating to Zr ion beam intensities were also conducted in order to ascertain the ideal running concentration of the sample solutions. A series of standard solutions were run at Zr concentrations of 200 ng mL^{-1}, 100 ng mL^{-1}, 50 ng mL^{-1} and 10 ng mL^{-1}. The results of these tests, shown in Fig. 5, indicate that the smallest uncertainty is associated with the 200 ng mL^{-1} solution (0.021‰, 2*sd*, $n = 10$), and that this error increases significantly when run at lower concentrations (e.g. 0.037‰ 2*sd*; $n = 10$ at [Zr] 100 ng mL^{-1} and 0.092‰ 2*sd*; $n = 10$ at [Zr] 50 ng mL^{-1}), which is in line with predictions of counting statistics. Furthermore it is apparent that the two solutions run at the lowest concentration are offset towards heavier values, similar to data reported by Schönbächler et al. (2004), which was attributed to an interference on ^{91}Zr. In light of this test all solutions analysed here were run at a concentration of 200 ng mL^{-1}.

4.3. Reproducible zirconium isotope measurements of natural samples

The precision of the method has been examined by processing and analysing six different whole rocks and one individual zircon. The results for all the natural samples analysed here are displayed in Fig. 6, with the exception of the Plešovice zircon grain, which is reported in Fig. 3. The data for these reference materials is provided in Table 2.

The external reproducibility of the method has been tested by repeating three separate dissolutions, column separations and measurements of BHVO-2. There is no resolvable offset between these three replicates (BHVO-2 [#1], BHVO-2 [#2] and BHVO-2 [#3]) and the individual mean values of the four separate analyses are consistent within < 0.015‰ of one another (Fig. 6). Based on these three repeats the compiled mean value of $\delta^{94/90}Zr_{IPGP\text{-}Zr}$ 0.044 ± 0.044‰ (2*sd*; $n = 12$), or ± 0.011‰/amu, for BHVO-2 is given.

In addition to the basalt BHVO-2, data for another basalt (JB-2), one andesite (AGV-2), two granites (GS-N and GA) and one serpentinite (UB-N) are presented. The basalt JB-2 displays a $\delta^{94/90}Zr_{IPGP\text{-}Zr}$ value of 0.053 ± 0.020‰ (2*sd*; $n = 4$), which is indistinguishable within

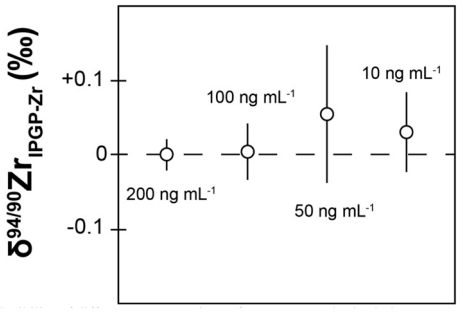

Fig. 5. The reproducibility of different concentrations of IPGP-Zr standard solutions. Uncertainties on individual measurements represents the 2sd of the mean where $n = 10$.

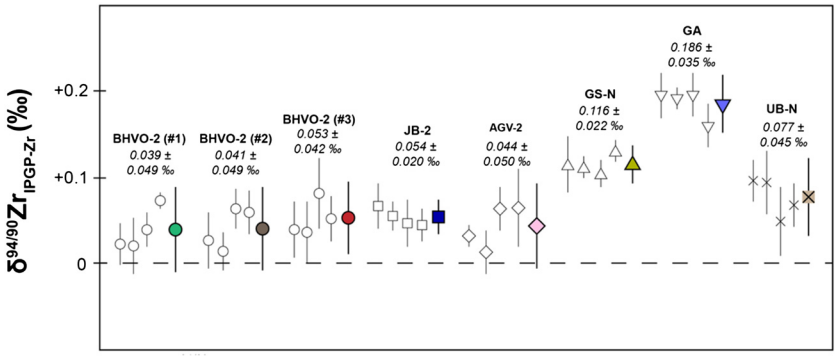

Fig. 6. The range of $\delta^{94/90}Zr_{IPGP\text{-}Zr}$ for all of the whole-rock samples analysed here. Hollow symbols represent individual sample analyses with the associated uncertainties being the internal 2 *se*. Filled bold symbols represents the average of the four measurements and the 2 *sd* uncertainty.

Table 2
A summary of the reference materials analysed as part of this study. The concentrations of Zr and SiO_2 are the certified values given by the USGS (for BHVO-2 and AGV-2), GSJ (for JB-2), CRPG SARM (for GS-N, GA and UB-N). The $\delta^{94/90}Zr_{IPGP\text{-}Zr}$ values given here represent the average of four individual sample measurements ($n = 4$) and the associated *2sd* of those measurements as the uncertainty.

Reference material	Dissolution method	[Zr] μg g^{-1}	[SiO_2] wt%	$\delta^{94/90}Zr_{IPGP\text{-}Zr}$ (‰)	± 2sd (‰)
BHVO-2 (#1)	Teflon bomb	172	49.9	0.039	0.049
BHVO-2 (#2)	Teflon bomb	172	49.9	0.041	0.049
BHVO-2 (#3)	Teflon bomb	172	49.9	0.053	0.042
Compiled BHVO-2 average				0.044	0.044
JB-2	Teflon bomb	50	53.3	0.054	0.020
AGV-2	Teflon bomb	230	59.3	0.044	0.050
GS-N	Teflon bomb	235	65.8	0.116	0.022
GA	Teflon bomb	150	69.9	0.186	0.035
GA	Parr bomb	150	69.9	0.188	0.019
UB-N	Teflon bomb	4	39.4	0.077	0.045
Plešovice zircon	Teflon bomb	–	–	0.106	0.043
Plešovice zircon	Parr bomb	–	–	0.113	0.033

uncertainty from BHVO-2. The andesitic sample AGV-2 displays a similar $\delta^{94/90}Zr_{IPGP\text{-}Zr}$ value to the two basaltic samples of 0.044 ± 0.050‰ (2*sd*; $n = 4$), while the two granites, GS-N and GA, are offset towards heavier $\delta^{94/90}Zr_{IPGP\text{-}Zr}$ values of 0.116 ± 0.022‰ and 0.186 ± 0.035‰ (2*sd*; $n = 4$ for both). The serpentinite, UB-N, has a $\delta^{94/90}Zr_{IPGP\text{-}Zr}$ value of 0.077 ± 0.045‰, which is lighter than the two granites but heavier than the basaltic and andesitic samples. The Plešovice zircon grain displays a $\delta^{94/90}Zr_{IPGP\text{-}Zr}$ value of 0.109 ± 0.037‰ (2*sd*; $n = 8$).

It is apparent that both significant and resolvable variation of Zr isotopes exits within terrestrial igneous rocks. Variations of different non-traditional stable isotopes systems have long been observed within igneous rocks and have been attributed to several different petrogenetic processes, such as: partial melting and melt extraction (e.g. Weyer and Ionov, 2007; Williams et al., 2009); magma redox processes (e.g. Sossi et al., 2012; Dauphas et al., 2014; Nebel et al., 2015); and fractional crystallization (e.g. Teng et al., 2008; Chen et al., 2013; Millet et al., 2016; Badullovich et al., 2017). Among the reference materials analysed here the more magmatically evolved display the heaviest isotopic composition. Considering this when the $\delta^{94/90}Zr_{IPGP\text{-}Zr}$ of the magmatic rocks are plotted against [SiO_2] (Fig. 7), it is apparent that samples with SiO_2 contents > 60 wt% display the heaviest $\delta^{94/90}Zr_{IPGP\text{-}Zr}$ values, thus Zr isotopes appear to be fractionated during igneous processes. At this

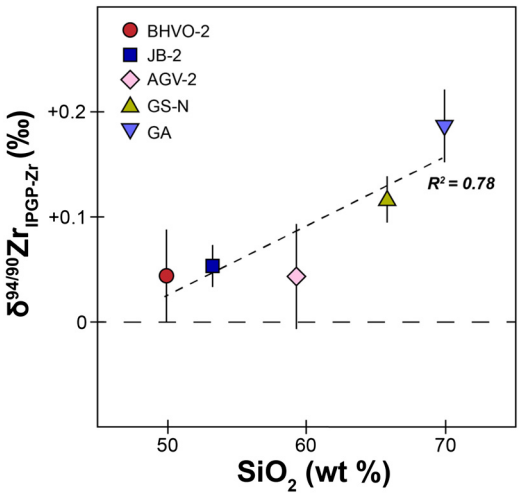

Fig. 7. The relationship between $\delta^{94/90}Zr_{IPGP\text{-}Zr}$ and SiO_2 content of the magmatic rocks analysed as part of this study. The SiO_2 content is taken from the certified values of each of the reference materials.

stage it is unclear as to the exact mechanism for this isotopic fractionation but because only the samples with SiO_2 contents > 60 wt% display markedly heavy isotopic compositions, then it is possible that this variation relates to the crystallization of an isotopically heavy phase during the later stages of magma differentiation. Since the rocks analysed here do not have a common magmatic source, it is impossible to exclude possible variations in the source composition. Further work must be done on differentiation series from a common source to test this effect. In any case, these results suggest that Zr isotopes may be used as tracers for igneous differentiation and crustal extraction. In particular, it may be possible to measure the Zr isotopic composition of individual zircon grains to attempt to evaluate the evolution of the Zr isotopic composition of the source through time, ultimately linking this to the dynamics of crustal extraction.

5. Conclusions

- A new method is presented for the determination of stable Zr isotopes within natural samples using a two step ion exchange chromatography with AG1-X8 and DGA resins, and analysis by MC-ICPMS using a ^{91}Zr–^{96}Zr double-spike to correct for mass discrimination.
- The chemical purification method effectively separates Zr from the sample matrix, including Mo, and we demonstrate that the purity of Zr in the processed samples is suitable for accurate determination of isotope ratios using the ^{91}Zr–^{96}Zr double-spike method.
- The method has an external reproducibility on $\delta^{94/90}Zr_{IPGP\text{-}Zr}$ in

silicate samples of ± 0.044‰ (2*sd*), or ± 0.011‰/amu.

- Six whole rock reference materials of varying bulk chemistries alongside a zircon reference grain show variations in $\delta^{94/90}Zr_{IPGP\text{-}Zr}$ on the order of 0.15‰, which is resolvable within uncertainties. The variation observed within the magmatic rocks see the samples with the highest SiO_2 content displaying the heaviest Zr isotope composition, thus suggesting that magmatic processes can fractionate Zr isotopes.

Supplementary data to this article can be found online at https://doi.org/10.1016/j.chemgeo.2018.07.007.

Acknowledgements

We thank the two anonymous reviewers for their thoughtful comments that have greatly clarified the manuscript and Klaus Mezger for efficient editorial handling. Funding for this work comes from the European Research Council [ERC Starting grant *PRISTINE*: 637503]. Pascale Louvat and Thibaut Sontag are acknowledged for technical support of the multi-collector facility at IPGP. Marc-Alban Millet (Cardiff) is thanked for discussion regarding double-spike and also for providing some of the reference materials. Jiří Sláma (Czech Academy of Sciences) is thanked for supplying the Plešovice zircon grains.

References

Akram, W., Schönbächler, M., 2016. Zirconium isotope constraints on the composition of Theia and current Moon-forming theories. Earth Planet. Sci. Lett. 449, 302–310.
Arnold, T., Schönbächler, M., Rehkämper, M., Dong, S., Zhao, F.J., Kirk, G.J., Coles, B.J., Weiss, D.J., 2010. Measurement of zinc stable isotope ratios in biogeochemical matrices by double-spike MC-ICPMS and determination of the isotope ratio pool available for plants from soil. Anal. Bioanal. Chem. 398, 3115–3125.
Badullovich, N., Moynier, F., Creech, J., Teng, F.Z., Sossi, P.A., 2017. Tin isotopic fractionation during igneous differentiation and Earth's mantle composition. Geochem. Perspect. Lett. 5, 24–28.
Berglund, M., Wieser, M.E., 2011. Isotopic compositions of the elements 2009 (IUPAC technical report). Pure Appl. Chem. 83, 397–410.
Bonnand, P., Parkinson, I.J., James, R.H., Karjalainen, A.M., Fehr, M.A., 2011. Accurate and precise determination of stable Cr isotope compositions in carbonates by double spike MC-ICP-MS. JAAS 26, 528–535.
Boulyga, S.F., Becker, J.S., 2001. ICP–MS with hexapole collision cell for isotope ratio measurements of Ca, Fe, and Se. Fresenius J. Anal. Chem. 370, 618–623.
Carlson, R.W., Hauri, E.H., Alexander, C.M.O.D., 2001. Matrix induced isotopic mass fractionation in the ICP-MS. In: Holland, J.G., Tanner, S.D. (Eds.), Plasma Source Mass Spectrometry: The New Millennium. The Royal Society of Chemistry, Cambridge, pp. 288–297.
Chaussidon, M., Deng, Z., Villeneuve, J., Moureau, J., Watson, B., Richter, F., Moynier, F., 2017. In situ analysis of non-traditional isotopes by SIMS and LA–MC–ICP–MS: key aspects and the example of Mg isotopes in olivines and silicate glasses. Rev. Mineral. Geochem. 82 (1), 127–163.
Chen, H., Savage, P.S., Teng, F.Z., Helz, R.T., Moynier, F., 2013. Zinc isotope fractionation during magmatic differentiation and the isotopic composition of the bulk Earth. Earth Planet. Sci. Lett. 369, 34–42.
Compston, W., Oversby, V.M., 1969. Lead isotopic analysis using a double spike. JGR 74, 4338–4348.
Creech, J.B., Paul, B., 2015. IsoSpike: improved double-spike inversion software. Geostand. Geoanal. Res. 39 (1), 7–15.
Creech, J., Baker, J., Handler, M., Schiller, M., Bizzarro, M., 2013. Platinum stable isotope ratio measurements by double-spike multiple collector ICPMS. JAAS 28, 853–865.
Creech, J.B., Moynier, F., Badullovich, N., 2017. Tin stable isotope analysis of geological materials by double-spike MC-ICPMS. Chem. Geol. 457, 61–67.
Cumming, G.L., 1973. Propagation of experimental errors in lead isotope ratio measurements using the double spike method. Chem. Geol. 11, 157–165.
Dauphas, N., Craddock, P.R., Asimow, P.D., Bennett, V.C., Nutman, A.P., Ohnenstetter, D., 2009. Iron isotopes may reveal the redox conditions of mantle melting from Archean to present. Earth Planet. Sci. Lett. 288, 255–267.
Dauphas, N., Roskosz, M., Alp, E.E., Neuville, D.R., Hu, M.Y., Sio, C.K., Tissot, F.L.H., Zhao, J., Tissandier, L., Médard, E., Cordier, C., 2014. Magma redox and structural controls on iron isotope variations in Earth's mantle and crust. Earth Planet. Sci. Lett. 398, 127–140.
Deng, Z., Moynier, F., van Zuilen, K., Sossi, P.A., Pringle, E.A., Chaussidon, M., 2018. Lack of resolvable titanium stable isotopic variations in bulk chondrites. Geochim. Cosmochim. Acta. https://doi.org/10.1016/j.gca.2018.06.016.
Dodson, M.H., 1970. Simplified equations for double-spiked isotopic analyses. Geochim. Cosmochim. Acta 34, 1241–1244.
Gale, N.H., 1970. A solution in closed form for lead isotopic analysis using a double spike. Chem. Geol. 6, 305–310.
Gall, L., Williams, H., Siebert, C., Halliday, A., 2012. Determination of mass-dependent variations in nickel isotope compositions using double spiking and MC-ICPMS. JAAS 21, 137–145.
Galy, A., Belshaw, N.S., Halicz, L., O'Nions, R.K., 2001. High-precision measurement of magnesium isotopes by multiple collector inductively coupled plasma-mass spectrometry. Int. J. Mass Spectrom. 208, 89–98.
Gopalan, K., MacDougall, D., Macisaac, C., 2006. Evaluation of a ^{42}Ca–^{43}Ca double-spike for high precision Ca isotope analysis. Int. J. Mass Spectrom. 248, 9–16.
Greber, N.D., Dauphas, N., Puchtel, I.S., Hofmann, B.A., Arndt, N.T., 2017a. Titanium stable isotopic variations in chondrites, achondrites and lunar rocks. Geochim. Cosmochim. Acta 213, 534–552.
Greber, N.D., Dauphas, N., Bekker, A., Ptáček, M.P., Bindeman, I.N., Hofmann, A., 2017b. Titanium isotopic evidence for felsic crust and plate tectonics 3.5 billion years ago. Science 357, 1271–1274.
Hopp, T., Fischer-Gödde, M., Kleine, T., 2016. Ruthenium stable isotope measurements by double spike MC-ICPMS. JAAS 31, 1515–1526.
Iizuka, T., Lai, Y.J., Akram, W., Amelin, Y., Schönbächler, M., 2016. The initial abundance and distribution of 92Nb in the Solar System. Earth Planet. Sci. Lett. 439, 172–181.
Ingle, C.P., Sharp, B.L., Horstwood, M.S., Parrish, R.R., Lewis, D.J., 2003. Instrument response functions, mass bias and matrix effects in isotope ratio measurements and semi-quantitative analysis by single and multi-collector ICP-MS. J. Anal. At. Spectrom. 18 (3), 219–229.
Kelemen, P.B., 1990. Reaction between ultramafic rock and fractionating basaltic magma I. Phase relations, the origin of calc-alkaline magma series, and the formation of discordant dunite. J. Pet. 31, 51–98.
Kleinhanns, I.C., Kreissig, K., Kamber, B.S., Meisel, T., Nägler, T.F., Kramers, J.D., 2002. Combined chemical separation of Lu, Hf, Sm, Nd, and REEs from a single rock digest: precise and accurate isotope determinations of Lu − Hf and Sm − Nd using multi-collector-ICPMS. Anal. Chem. 74, 67–73.
May, T.W., Wiedmeyer, R.H., 1998. A table of polyatomic interferences in ICP-MS. At. Spectrosc. Norwalk Conn. 19, 150–155.
McCoy-West, A.J., Millet, M.A., Burton, K.W., 2017. The neodymium stable isotope composition of the silicate Earth and chondrites. Earth Planet. Sci. Lett. 480, 121–132.
McDonough, W.F., Sun, S.-S., 1995. Composition of the Earth. Chem. Geol. 120, 223–253. https://doi.org/10.1016/0009-2541(94)00140-4.
Mead, C., Johnson, T.M., 2010. Hg stable isotope analysis by the double-spike method. Anal. Bioanal. Chem. 397, 1529–1538.
Millet, M.A., Dauphas, N., 2014. Ultra-precise titanium stable isotope measurements by double-spike high resolution MC-ICP-MS. JAAS 29, 1444–1458.
Millet, M.A., Baker, J.A., Payne, C.E., 2012. Ultra-precise stable Fe isotope measurements by high resolution multiple-collector inductively coupled plasma mass spectrometry with a ^{57}Fe–^{58}Fe double spike. Chem. Geol. 304, 18–25.
Millet, M.A., Dauphas, N., Greber, N.D., Burton, K.W., Dale, C.W., Debret, B., Macpherson, C.G., Nowell, G.M., Williams, H.M., 2016. Titanium stable isotope investigation of magmatic processes on the Earth and Moon. Earth Planet. Sci. Lett. 449, 197–205.
Nanne, J.A., Millet, M.A., Burton, K.W., Dale, C.W., Nowell, G.M., Williams, H.M., 2017. High precision osmium stable isotope measurements by double spike MC-ICP-MS and N-TIMS. JAAS 32, 749–765.
Navarro, M.S., Andrade, S., Ulbrich, H., Gomes, C.B., Girardi, V.A., 2008. The direct determination of rare earth elements in basaltic and related rocks using ICP-MS: testing the efficiency of microwave oven sample decomposition procedures. Geostand. Geoanal. Res. 32, 167–180.
Nebel, O., Sossi, P.A., Benard, A., Wille, M., Vroon, P.Z., Arculus, R.J., 2015. Redox-variability and controls in subduction zones from an iron-isotope perspective. Earth Planet. Sci. Lett. 432, 142–151.
Niu, Y., 1997. Mantle melting and melt extraction processes beneath ocean ridges: evidence from abyssal peridotites. J. Pet. 38, 1047–1074.
Niu, Y., 2004. Bulk-rock major and trace element compositions of abyssal peridotites: implications for mantle melting, melt extraction and post-melting processes beneath mid-ocean ridges. J. Pet. 45, 2423–2458.
Rehkämper, M., Wombacher, F., Aggarwal, J.K., 2004. Stable isotope analysis by multiple collector ICP-MS. In: Handbook of Stable Isotope Analytical Techniques. Volume I. pp. 692–725.
Rollinson, H., 1993. Using geochemical data: Evaluation, Presentation, Interpretation. Longman Scientific & Technical, pp. 352.
Ronov, A.B., Yaroshevsky, A.A., 1969. Chemical composition of the earth's crust. In: The Earth's Crust and Upper Mantle, pp. 37–57.
Rudge, J.F., Reynolds, B.C., Bourdon, B., 2009. The double spike toolbox. Chem. Geol. 265, 420–431.
Russell, R.D., 1971. The systematics of double spiking. JGR 76, 4949–4955.
Salters, V.J.M., 1998. Elements: High field strength. In: Geochemistry. Springer, Netherlands, pp. 209–210.
Salters, V.J.M., Shimizu, N., 1988. World-wide occurrence of HFSE-depleted mantle. Geochim. Cosmochim. Acta 52, 2177–2182.
Schoenberg, R., Zink, S., Staubwasser, M., Von Blanckenburg, F., 2008. The stable Cr isotope inventory of solid Earth reservoirs determined by double spike MC-ICP-MS. Chem. Geol. 249, 294–306.
Schönbächler, M., Rehkämper, M., Lee, D.C., Halliday, A.N., 2004. Ion exchange chromatography and high precision isotopic measurements of zirconium by MC-ICP-MS. Analyst 129, 32–37.
Shiel, A.E., Barling, J., Orians, K.J., Weis, D., 2009. Matrix effects on the multi-collector inductively coupled plasma mass spectrometric analysis of high-precision cadmium and zinc isotope ratios. Anal. Chim. Acta 633 (1), 29–37.
Siebert, C., Nägler, T.F., Kramers, J.D., 2001. Determination of molybdenum isotope

fractionation by double-spike multicollector inductively coupled plasma mass spectrometry. Geochem. Geophys. Geosyst. https://doi.org/10.1029/2000GC000124.
Siebert, C., Ross, A., McManus, J., 2006. Germanium isotope measurements of high-temperature geothermal fluids using double-spike hydride generation MC-ICP-MS. Geochim. Cosmochim. Acta 70, 3986–3995.
Sláma, J., Košler, J., Condon, D.J., Crowley, J.L., Gerdes, A., Hanchar, J.M., Horstwood, M.S., Morris, G.A., Nasdala, L., Norberg, N., Schaltegger, U., 2008. Plešovice zircon—a new natural reference material for U–Pb and Hf isotopic microanalysis. Chem. Geol. 249, 1–35.
Sossi, P.A., Foden, J.D., Halverson, G.P., 2012. Redox-controlled iron isotope fractionation during magmatic differentiation: an example from the Red Hill intrusion, S. Tasmania. Contrib. Mineral. Petrol. 164, 757–772.
von Strandmann, P.A.P., Coath, C.D., Catling, D.C., Poulton, S.W., Elliott, T., 2014. Analysis of mass dependent and mass independent selenium isotope variability in black shales. JAAS 29, 1648–1659.
Teng, F.Z., Dauphas, N., Watkins, J.M., 2017. Non-traditional stable isotopes: retrospective and prospective. Rev. Mineral. Geochem. 82, 1–26.
Teng, F.Z., Dauphas, N., Helz, R.T., 2008. Iron isotope fractionation during magmatic differentiation in Kilauea Iki lava lake. Science 320 (5883), 1620–1622.
van Westrenen, W., Blundy, J.D., Wood, B.J., 2001. High field strength element/rare earth element fractionation during partial melting in the presence of garnet: implications for identification of mantle heterogeneities. Geochem. Geophys. Geosyst. 2. https://doi.org/10.1029/2000GC000133.
Weyer, S., Schwieters, J.B., 2003. High precision Fe isotope measurements with high mass resolution MC-ICPMS. Int. J. Mass Spectrom. 226, 355–368.
Weyer, S., Münker, C., Mezger, K., 2003. Nb/Ta, Zr/Hf and REE in the depleted mantle: implications for the differentiation history of the crust–mantle system. Earth Planet. Sci. Lett. 205, 309–324.
Weyer, S., Ionov, D.A., 2007. Partial melting and melt percolation in the mantle: the message from Fe isotopes. Earth Planet. Sci. Lett. 259 (1-2), 119–133.
Weyer, S., Anbar, A.D., Gerdes, A., Gordon, G.W., Algeo, T.J., Boyle, E.A., 2008. Natural fractionation of 238U/235U. Geochim. Cosmochim. Acta 72, 345–359.
Williams, H.M., Nielsen, S.G., Renac, C., Griffin, W.L., O'Reilly, S.Y., McCammon, C.A., Pearson, N., Viljoen, F., Alt, J.C., Halliday, A.N., 2009. Fractionation of oxygen and iron isotopes by partial melting processes: implications for the interpretation of stable isotope signatures in mafic rocks. Earth Planet. Sci. Lett. 283 (1), 156–166.
Winchester, J.A., Floyd, P.A., 1977. Geochemical discrimination of different magma series and their differentiation products using immobile elements. Chem. Geol. 20, 325–343.
Woodhead, J., Eggins, S., Gamble, J., 1993. High field strength and transition element systematics in island arc and back-arc basin basalts: evidence for multi-phase melt extraction and a depleted mantle wedge. Earth Planet. Sci. Lett. 114, 491–504.
Xue, Zichen, Rehkämper, Mark, Schönbächler, Maria, Statham, Peter J., Coles, Barry J., 2012. A new methodology for precise cadmium isotope analyses of seawater. Anal. Bioanal. Chem. 402 (2), 883–893.